

Environmental controls on evapotranspiration from sparse grassland in Mongolia

Yinsheng Zhang,^{1*} T. Kadota,¹ T. Ohata¹ and D. Oyunbaatar²

¹ Institute of Observational Research for Global Change, Yokosuka 237-0061, Japan

² Institute of Meteorology and Hydrology, Ulaanbaatar, Mongolia

Abstract:

Environmental controls on evapotranspiration were investigated at a sparse grassland in Mongolia during 2003 and 2004. The study site was located on the southern periphery of the Eurasian cryosphere. Data from Eddy covariance, aerodynamic, and manual measurements were used in the analysis. A decoupling factor (Ω) was calculated to determine the relative importance of surface conductance and radiation to change in evapotranspiration rates. Higher evapotranspiration rates associated with a higher frequency of large Ω values revealed the importance of radiation forcing on evapotranspiration at this study site. As Ω increases, the aerodynamic conductance (g_a) increased correspondingly but vegetation conductance (g_c) decreased. Aerodynamic conductance (g_a) was well fitted to an exponential function of the wind stress; g_c clearly decreased as the vapour pressure deficit (d) increased; g_c related to air temperature through d . Although grass cover was sparse at the study site, the anticipated effect of soil moisture on E and g_s was only slightly suggested and thus not deducible. On the 10-day-interval time scale, the effect of vegetation cover on evapotranspiration was insignificant compared to that of surface soil moisture. Changes in soil evaporation, related to precipitation, mainly caused the very large inter-annual differences in evapotranspiration. The relationship between evapotranspiration and surface bulk resistance at the study site could therefore be fit to an exponential function. Copyright © 2007 John Wiley & Sons, Ltd.

KEY WORDS evapotranspiration; grassland; conductance; Mongolia

Received 1 July 2005; Accepted 1 February 2006

INTRODUCTION

Evapotranspiration is an important physical process controlled by a number of interconnected environmental and biological factors (Jarvis and McNaughton, 1986; Wilson and Baldocchi, 2000). In recent decades, evapotranspiration from the land surface has been seen as a key component of the water cycle. Evapotranspiration links energy partitioning, stomatal conductance, carbon exchange, and water-use efficiency in plant communities and serves as a key regulator of the ecosystem processes (Woodward and Smith, 1994; Sellers *et al.*, 1996). In particular, when considering the effects of global climate change, evapotranspiration represents the interaction between vegetation and the atmosphere. Variation of evapotranspiration is influenced by all ecosystem parameters and processes, such as soil moisture content, vegetation productivity, and ecosystem nutrient and water budgets. The partitioning of available energy into evapotranspiration (latent heat flux) and sensible heat flux at a vegetation surface also affects aspects of weather and climate (Dirmeyer, 1994; Pielke *et al.*, 1998). There has been great interest, therefore, in studying evapotranspiration in a variety of ecosystems to better understand the nature of the

controlling interactions and the links between evapotranspiration and other earth system processes.

Today, we have a fairly sound understanding of the mechanisms that control transpiration, or stomatal conductance of plants, from potometer (or chamber) measurements (e.g. Shuttleworth and Wallace, 1985; Jones, 1992). Recent studies based on micrometeorological measurements (e.g. Steduto and Hsiao, 1998; Villalobos *et al.*, 2000) and model applications (e.g. Alves and Pereira, 2000; Calvet, 2000; Mo and Liu, 2001) have also clarified evapotranspiration processes. Over the past decade, international study programs such as the Global Energy and Water Cycle Experiment/Asian Monsoon Experiment (GEWEX/GAME) and the International Geosphere-Biosphere Programme (IGBP)/FLUXNET have also reported significant findings. However, applying these findings to climate models remains a challenge. Specifically, appropriate up-scaling from leaf to plant, from plant to canopy, and from canopy to landscape must be addressed. The processes controlling evapotranspiration and energy partitioning over an entire vegetation community also require further clarification (Grelle *et al.*, 1999), as do seasonal dynamics, in which phenology and variations in soil moisture and temperature play important roles (Viterbo and Beljaars, 1995).

Grassland ecosystems offer special opportunities to study the response of ecosystem physiology to environmental change. Knapp and Smith (2001), for instance,

* Correspondence to: Yinsheng Zhang, Institute of Observational Research for Global Change, Japan Agency for Marine-Earth Science and Technology (IORGC/JAMSTEC), 2-15 Natsushima-cho, Yokosuka, 237-0061, Japan. E-mail: yszhang@jamstec.go.jp

found that grasslands had the largest inter-annual variation in primary production among the major ecosystems in the continental U.S.; these variations were primarily produced by changes in precipitation and may thus be the most responsive to future climatic changes. Grasslands in that study also exhibited very large asymmetric responses to annual variation in precipitation. Increases in productivity in wet years were much more pronounced than reductions in productivity during drought years (Knapp and Smith, 2001). These asymmetric responses may have been due to characteristics of grassland plants that allow them to resist drought and then quickly generate new growth when moisture becomes available. Because of the strong link between vegetation productivity and evapotranspiration (Schulze *et al.*, 1994), a large inter-annual variation can also be expected in evapotranspiration. Flanagan *et al.* (2002) examined this issue in their study of carbon dioxide exchange in grasslands.

Grassland vegetation covers more than 80% of Mongolia. Ma *et al.* (2003) have defined northeastern Mongolia as semi-arid with high potential evapotranspiration and a low wetness index. Relatively few studies of evapotranspiration have been conducted in semi-arid environments (Shirley and Eric, 2004). Those limited field studies that have examined semi-arid environments have shown wide temporal variations in evapotranspiration. However, because precipitation is much lower than potential evapotranspiration in arid and semi-arid environments, evapotranspiration is believed to be limited by soil moisture and the presence of dry-land ecosystems (Noy-Meir, 1973; Rodriguez-Iturbe, 2000). Both simple and complex hydrologic models typically include the dependence of evapotranspiration on soil moisture and ecosystem type (Desborough *et al.*, 1996; Mahfouf *et al.*, 1996). Unfortunately, the field data required to test these relationships are often lacking, particularly, for arid and semi-arid environments where limitations arising from low soil moisture are believed to be most important.

To help address this gap in the literature, the present study analysed Eddy covariance and aerodynamic measurements of evapotranspiration and energy flux taken over a sparse grassland site along the southern periphery of the Eurasian cryosphere in Mongolia. The evaluation period covered two full years (2003 and 2004). We applied the decoupling technique of Jarvis and McNaughton (1986) to analyse the effect of environmental factors on surface conductance in the study years; this method allowed us to assess the biological and environmental factors, which controlled evapotranspiration and surface conductance in this northern grassland.

MATERIALS AND METHODS

Site descriptions

An observation site was established on sparse grassland at Nalaikh in northeastern Mongolia (47°45'N, 107°20'E) 40 km southeast of Ulaanbaatar. The site was located on a sediment plain in the broad Tuul River valley (Figure 1).

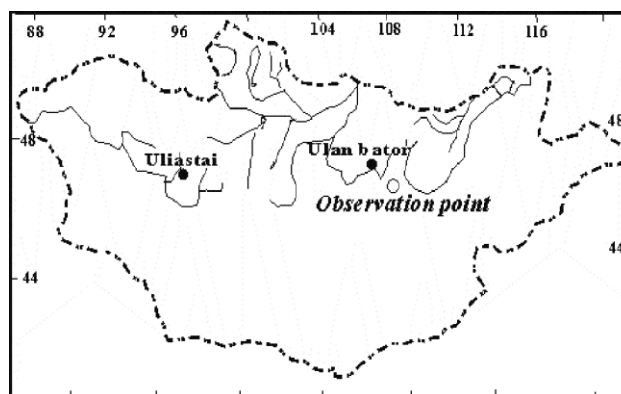


Figure 1. Location of the study site

The nearest mountains, with relative heights of less than 500 m, were at least 10 km away, and the topography at and around this site was very smooth.

The observation site was in a semi-arid region characterized by warm, dry summers (Bereneva, 1992). Figure 2 presents monthly precipitation and air temperatures for 2003 and 2004 and mean values from 1980 to 2004 at Ulaanbaatar station, 40 km west of the study site. The summer air temperature (June to August) was higher than average at 0.7 °C in 2003 and 2.3 °C in 2004. Precipitation in the growing season (May to September) averaged 224.9 mm from 1980 to 2004 was 246.9 mm and 190.4 mm in 2003 and 2004, implying a moister than usual summer in 2003 and a drier than usual summer in 2004.

The surface soil in the study region is sandy, contains little organic matter, and is less than 10 cm thick. Large sand grains occur beneath the organic layer with a bulk density of 1.1–1.7 g cm⁻³ and porosity of 32–59%. The observation site was located at the periphery of the sub-Arctic permafrost region (Sharkhuu, 2001). A thick active layer and higher ground surface temperatures characterize permafrost regions. Observations of ground temperature from the surface to a depth of 3 m showed that the surface temperature was continuously below 0 °C at the beginning of October. The downward frost front moved from the surface to 3 m in the following 85–90 days. After the snowcover disappeared at the beginning of April, the surface started to melt. The downward-moving thawing front reached 3 m at the end of April. Seasonal variation of the permafrost active layer suggests that the thaw–frost cycle may not affect biological processes of the grass, because the thaw depth exceeded 3 m during the growth period (May to September), even though the study site was underlain by permafrost. Therefore, this situation can be classified as ‘warm permafrost’ (Ishikawa *et al.*, 2005a).

Vegetation was uniformly sparse grass covering 38–60% of the land surface during the maximum growth period. Plant type and species showed little variation; *Artemisia frigida* was dominant (~60%) with other species including *Arenaria* and *Leymus chinensis*. The maximum grass height in mid-July was less than 20 cm.

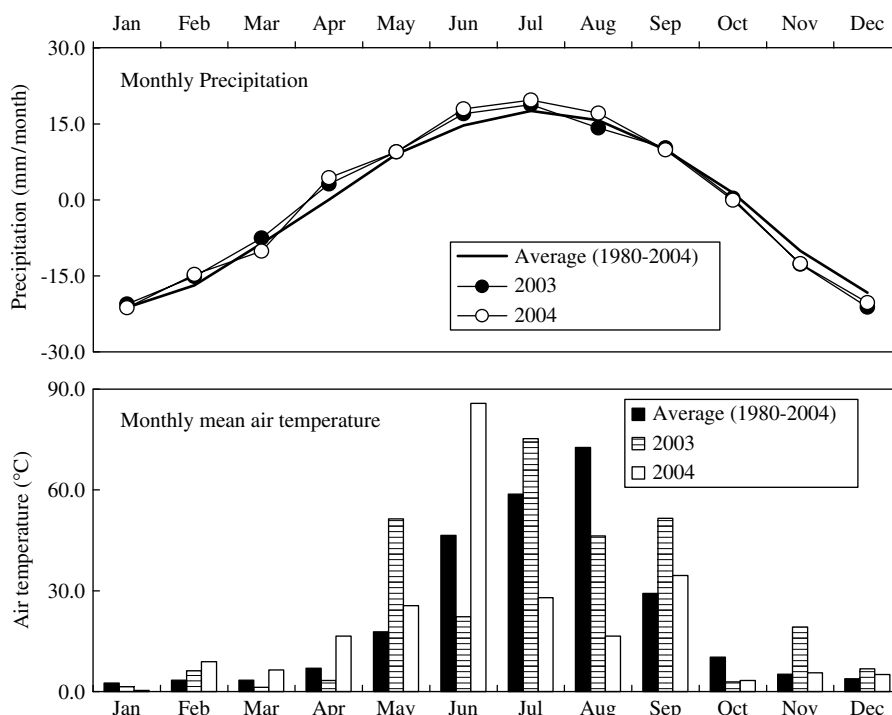


Figure 2. Monthly precipitation, air temperatures for 2003 and 2004, and mean curve of air temperatures from 1980 to 2004 at the Ulaanbaatar station, 40 km west of the study site

Table I. Instruments used in this study

Item	Unit	Instrument (model, manufacturer)	Record interval
Short-wave radiation	Wm^{-2}	Radiometer (MS402, EKO, Japan)	10 min
Long-wave radiation	Wm^{-2}	Infrared radiometer (MS202, EKO, Japan)	10 min
All-wave net radiation	Wm^{-2}	Net radiometer (REBS Q7, REBS, Inc., USA)	10 min
Photosynthetically active radiation (PAR)	$\mu\text{Es}^{-1} \text{m}^{-2}$	Optical photon meter (PAR-01, REBS, Inc., USA)	10 min
Wind speed	ms^{-1}	Anemometer (AC750, Kaijo Corporation, Japan)	10 min
Wind direction	deg	Anemometer (VR036, Kaijo Corporation, Japan)	10 min
Snow depth	cm	Ultrasonic level-meter (SR50, Kaijo Corporation, Japan)	60 min
Precipitation	mm	Tipping bucket rain gauge (52 202, R. M. Young Co., USA)	10 min
Air temperature	$^{\circ}\text{C}$	Humidity and temperature probe (HMD45D, Vaisala Oyj, Finland) with ventilation pipe (PVC-02, PREDE, Japan)	10 min
Relative humidity	%	Humidity and temperature probe (HMD45D, Vaisala Oyj, Finland) with ventilation pipe (PVC-02, PREDE, Japan)	10 min
Surface temperature	$^{\circ}\text{C}$	Infrared radiation thermometer (CML303F, CLIM., Inc., Japan)	10 min
Heat flux in the soil	Wm^{-2}	Heat flux plate (PHF01, REBS, Inc., USA)	10 min
Volumetric water content	m^3/m^3	ECHO probe (EC-10, Decagon Devices, Inc. USA)	10 min
Soil temperature	$^{\circ}\text{C}$	Pt-thermometer (TPT100S, CLIMATEC, Inc., Japan)	10 min
Air pressure	hPa	Analog barometer (PTB101B, Vaisala Oyj, Finland)	10 min
Friction wind velocity	m/s	Ultrasonic Anemometer (Kaijo Corporation, Japan)	10 min
Latent and sensible heat	Wm^{-2}	Ultrasonic Anemometer (Kaijo Corporation, Japan)	10 min

Observations

An automatic climate observation system (ACOS) recorded air temperature, humidity, and wind speed at heights of 0.5, 1.0, 2.0, and 4.0 m. Short-wave radiation, long-wave radiation, and photosynthetically active radiation (PAR) were measured in both upward and downward directions. In addition, sensors measuring air pressure and an infrared radiation thermometer recording grass leaf temperature and net radiation were installed 1.5 m above the ground surface. The Eddy covariance

method was used to measure latent heat (Q_E), sensible heat (Q_H), and friction wind speed (u^*) at 2 m above the ground. We used an open-path hygrometer/ H_2O sensor (KH20, Campbell, USA) and a three-dimensional supersonic anemometer (81 000, YOUNG, USA). Table I provides details of other instruments used in this study. The data presented below were collected during the two study years (2003–2004), however, the Eddy covariance measurement was conducted just during the grass growth period of 2004. Therefore, aerodynamics is the main

method to present full seasonal variation of heat/vapour fluxes at the study site. The parameters estimation in aerodynamics formulas were achieved from result of Eddy covariance measurement as show in following section.

Precipitation gauges often underestimate true precipitation amounts. Zhang *et al.* (2004) estimated the downward bias of gauge-measured annual precipitation to be between 17 and 42% in Mongolia. Yokoyama *et al.* (2003) detailed the bias of the gauge used in this study; our precipitation data have been corrected using their procedure, which anticipated a bias of 17%.

Soil moisture was observed both automatically and manually. Seven time-domain reflectometry (TDR) probes and seven Pt thermometers were installed at depths of 0, 0.2, 0.4, 0.8, 1.2, 2.4, and 3.0 m; two sets of heat flux meters were also inserted at 0.02 and 0.2 m. Along with a data logger, these sensors comprised the soil monitoring system (SMS). Soil moisture in the surface layer (0–60 cm) was also manually sampled to calibrate the TDR data.

Phenology observations included the grass coverage and biomass and the water content of grass leaves. These observations were conducted at 10-day intervals from July 2002 to June 2004 and were conducted at four 50 × 50 cm plots. The results shown are averages from the four plots.

Data analysis

The heat budget during the snow-free period can be written as

$$Q_N = Q_H + Q_E + Q_G \tag{1}$$

Here, Q_N is the net radiation, Q_G is the ground energy flux, and Q_H and Q_E are the sensible and latent heat flux, respectively, which can be calculated by the aerodynamic method:

$$Q_H = \rho C_P C_H \Delta U \Delta T \tag{2}$$

$$Q_E = \rho L_E C_E \Delta U \Delta q \tag{3}$$

where C_P is the specific energy at constant pressure, L_E is the latent energy of vaporization, U is the wind speed, and T is the air temperature, q is the specific humidity. C_H and C_E are bulk transfer coefficients for heat and vapour, respectively, calculated as by Brutsaert (1984) as

$$C_H = k^2 \left[\ln\left(\frac{z_2}{z_1}\right) - \Psi_H \right]^{-1} \left[\ln\left(\frac{z_2}{z_1}\right) - \Psi_m \right]^{-1} \text{ and} \tag{4}$$

$$C_E = k^2 \left[\ln\left(\frac{z_2}{z_1}\right) - \Psi_W \right]^{-1} \left[\ln\left(\frac{z_2}{z_1}\right) - \Psi_m \right]^{-1}$$

where k is the von Karman constant (0.41), the subscripts 2 and 1 denote measurement levels, and Ψ_H , Ψ_w , and Ψ_m are stratification functions dependant on the Richardson number (Ri):

$$Ri = \frac{g}{T} \frac{\Delta T}{\Delta z} \left(\frac{\Delta U}{\Delta z} \right)^{-2} \tag{5}$$

In this study, Ψ_H , Ψ_w , and Ψ_m were deduced from Eddy covariance observations:

$$Ri > 0.17, \begin{cases} \Psi_H = 6.11 Ri / (1 - Ri) \\ \Psi_W = 1.22 \Psi_H \\ \Psi_m = \Psi_H \end{cases} \tag{6}$$

$$-0.35 < Ri \leq 0.17, \begin{cases} \Psi_H = \exp(1.12 Ri / (1 - Ri)) \\ \Psi_W = 1.22 \Psi_H \\ \Psi_m = \Psi_H \end{cases} \tag{7}$$

$$Ri \leq -0.35, \begin{cases} \Psi_H = \exp(10.63 Ri) \\ \Psi_W = 0.71 \Psi_H \\ \Psi_m = \Psi_H \end{cases} \tag{8}$$

To study the relative contribution of the radiation (E_{RAD}) and aerodynamic (E_{AERO}) terms to the overall evapotranspiration (E), Jarvis and McNaughton (1986) presented the following equation:

$$E = E_{RAD} + E_{AERO} = \Omega E_{eq} + (1 - \Omega) E_{im} \tag{9}$$

where E_{eq} is equilibrium evaporation that depends only on the energy supply (radiation). E_{im} is the part of the evapotranspiration imposed by the surrounding air. Ω is a dimensionless decoupling factor computed as

$$\Omega = (\delta + \gamma) / (\delta + (1 + g_a / g_c)) \tag{10}$$

where g_c and g_a are the ecosystem surface conductance and aerodynamic conductance, respectively, which can be calculated as follows (Monteith and Unsworth, 1990):

$$1/g_a = U/u^{*2} + 6.2u^{*-0.67} \tag{11}$$

$$1/g_c = \rho C_P d / (\gamma Q_E) + (\beta \delta / \gamma - 1) / g_a \tag{12}$$

$$E_{eq} = \frac{\delta}{\delta + \gamma} Q_{ne} \tag{13}$$

$$E_{im} = \rho C_P d g_c / (L_E \gamma) \tag{14}$$

where d is the vapour pressure deficit, δ is the slope of the saturation water vapour pressure curve, and γ is

$$\gamma = C_P P / 0.622 L_E \tag{15}$$

where P is air pressure. Q_{ne} is the heat energy available for evaporation, as determined by the net radiation (Q_N) and ground heat flux (Q_G):

$$Q_{ne} = (Q_N - Q_G) / L_E \tag{16}$$

The extractable soil water (ESW) is an effective indicator of soil water status in relation to plant growth. ESW was defined by Noilhan and Planton (1989) as

$$ESW = \frac{\theta - \theta_{WILT}}{\theta_{FC} - \theta_{WILT}} \tag{17}$$

where θ is the soil volumetric moisture in the root zone, and θ_{FC} and θ_{WILT} are the root-zone moisture content at field capacity and wilting point, respectively. In this study, the root zone was defined as 0–50 cm according to the root distribution. θ_{FC} and θ_{WILT} were 17.2 and 4.1%, respectively. Thus, ESW indicates the fractional plant–available-soil-water status, or relative soil water

content. The former was measured in the field, and the latter was determined in the laboratory. The soil water capacity ranged from 6.5 to 17.2%, and the wilting point ranged from 2.8 to 4.1% in the surface layer.

RESULTS

Performance of flux measurements and heat budget closure

Sensible and latent heat fluxes were measured by an Eddy covariance system. However, measurements by the Eddy covariance measurement were only conducted from 20 May to 28 August 2004 and failed to successfully record data on some rainy days. Therefore, sensible and latent heat fluxes calculated by aerodynamic formulas (2)–(5) to present full seasonal variation. Some parameters used in formulas (2)–(5) were deduced from the results of Eddy covariance measurement as shown in Equations (6)–(8). The sensible and latent heat fluxes gained by Eddy covariance and aerodynamic formulas are compared in the left panel of Figure 3 during the calibration period; each point shows the hourly mean. The regression slope was 0.948 for latent heat flux and 1.0823 for sensible heat flux. The calculated latent heat flux by the aerodynamic method was about 5% lower than that from the Eddy covariance measurement on average, but the calculated sensible heat flux was higher by about 7%. The agreement between the daily values from the two systems was good, giving credibility to the values from subsequent calculations.

Energy balance closure provides a check for calculations by aerodynamic formulas. The daily energy balance at the study site, i.e. the sum of the sensible and latent heat fluxes ($Q_H + Q_E$) versus the difference of net radiation and ground heat flux ($Q_N - Q_G$) during the snow-free periods of 2003 and 2004, is shown in the right panel of Figure 3 by hourly scale. The slope is less than 1 (0.976) with a coefficient of determination

(R^2) of 0.7724. The intercept of the sum of $Q_H + Q_E$ and $Q_N - Q_G$ was 8.01 Wm^{-2} (about 8% on average). The error between $Q_H + Q_E$ and $Q_N - Q_G$ might mainly cause by Q_G measurement, which was measured at the surface by the heat flux meter. Ishikawa *et al.* (2006) has demonstrated Q_G might be underestimated from soil thermal processes investigation at the same study site. They found significant heat consumption for soil internal vaporization within ground surface layer. It is clear that heat consumption cannot be measured by heat flux meter, which leads to overestimating $Q_N - Q_G$. From these findings, it could be concluded that the aerodynamic formulas and the improved parameter estimation used were adequate for continuing the analysis.

Meteorological and surface conditions during the study period (2003–2004)

Figure 4 shows the daily mean global radiation, albedo, surface soil moisture, air temperature, ground temperature at 1.2 m, and daily precipitation at the study site during 2003 and 2004. The annual mean global solar radiation flux was 175.3 Wm^{-2} . The average albedo was 0.71 during periods with snow cover and was 0.12 during periods without snow. Accordingly, the average net radiation for each period was -6.0 Wm^{-2} and 60.0 Wm^{-2} , respectively. The annual precipitation was 176.0 mm in 2003 and 147.5 in 2004; the corresponding annual mean air temperatures were -4.3 and -3.1 °C. The grass-growing season (May to September) received 79% of the annual precipitation. The annual mean relative humidity was 61%. The prevailing wind was from the NW–ENE with annual mean wind speed of 2.6 m/s. The wind was stronger (mean wind speed of 3.2 m/s) during the period of grass growth than that in other reasons.

Seasonal variation in grass phenology

Figure 5 shows the seasonal variation of grass coverage, water content in grass leaves, biomass, and the LAI

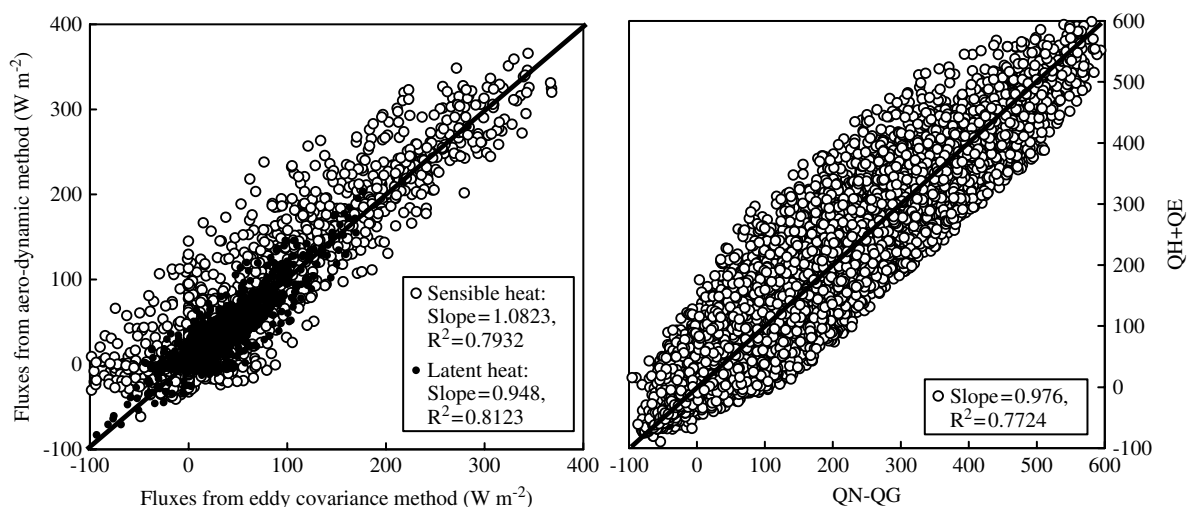


Figure 3. Relationship between the calculated heat fluxes by aerodynamic method and Eddy covariance measurement (left panel) from 20 May to 28 August 2004 and between the sum of $Q_H + Q_E$ versus $Q_N - Q_G$ at study site in the snow-free periods of 2003 and 2004. Each point shows the hourly mean

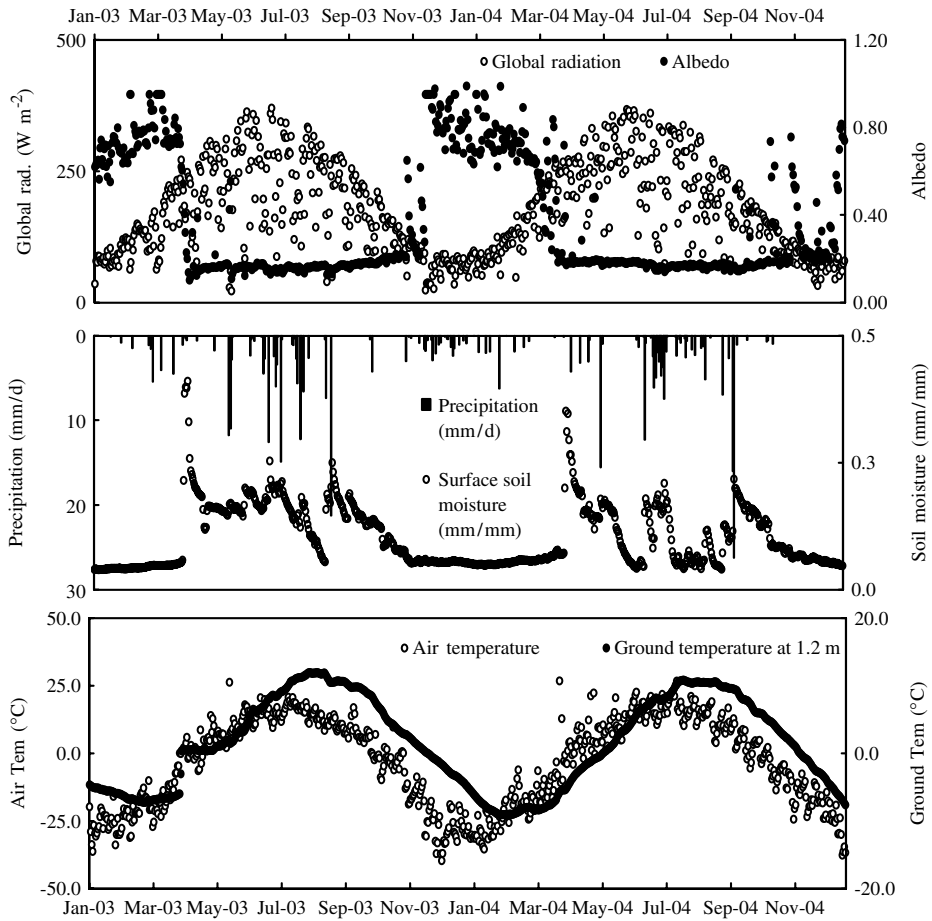


Figure 4. Daily mean global radiation, albedo, surface soil moisture, air temperature, and ground temperature at 1.2 m and daily precipitation at the study site

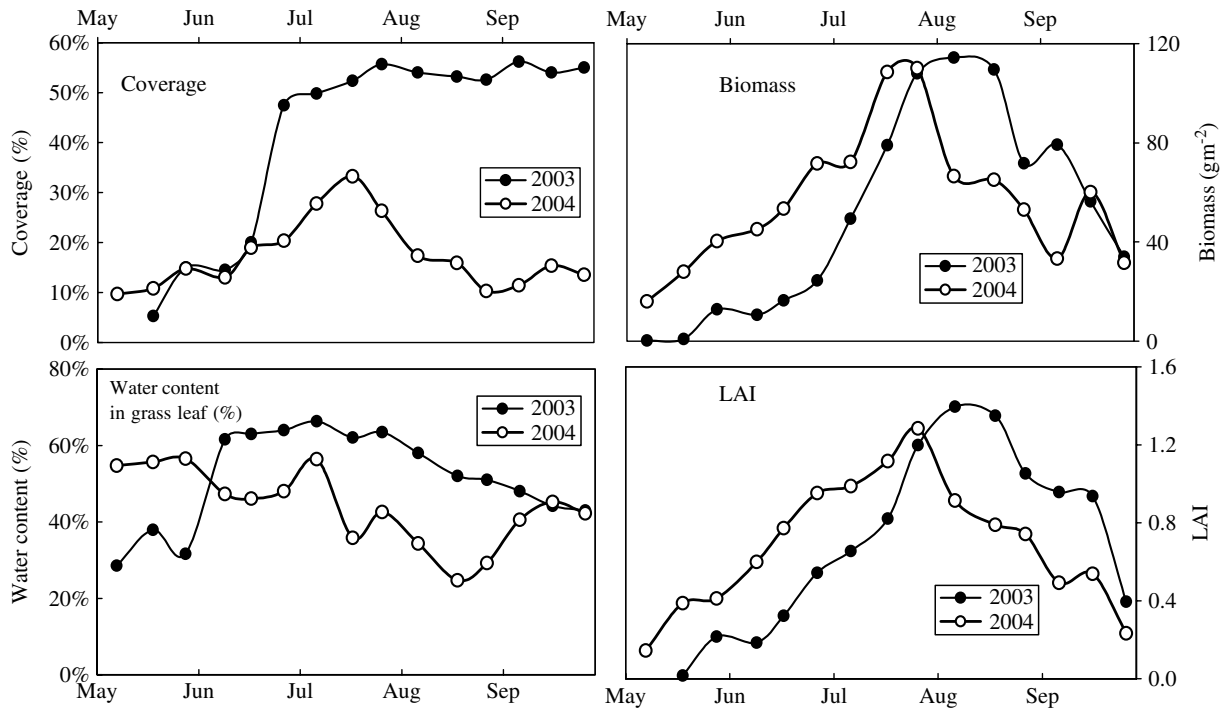


Figure 5. Seasonal variation of grass coverage, biomass, water content in grass leaf, and the LAI at the study site

over the two-year period. Grass began to become visible at the beginning of May and senesced at the end of September. The most significant difference at the inter-annual scale was found in the grass coverage, which was 55.7% in 2003, 20% higher than the maximum coverage in 2004. Although both the biomass and the LAI had rather low values due to the semi-arid climate, general seasonal variation could still be seen. Peak values of 110 gm^{-2} biomass and 1.25 LAI were measured at approximately mid-summer each year; these values were somewhat lower at the beginning of the growth period.

Seasonal patterns and partitions of the heat budget

To clarify the seasonal pattern and partitions of the heat budget, we examined seasonal variation in a 10-day mean net radiation (Q_N), sensible heat (Q_H), latent heat (Q_E), and ground heat flux (Q_G) at the study site during 2003 and 2004, as detailed in Figure 6 (upper panel). The 10-day mean values of the ratio of latent heat flux to net radiation (Q_E/Q_N) and the Bowen ratio (B_0) for the 2003 and 2004 growth periods are also shown in the lower panel of Figure 6. During the pre-growth periods from the time the snow disappeared until grass shoots could be seen (1–30 April 2003; 27 March–30 April 2004), values of Q_N , Q_H , and Q_G all increased. In contrast, less consistent changes were observed for Q_E . Values were rather high initially and later decreased sharply, with a mean value of 26.1 Wm^{-2} in 2003 and 12.8 Wm^{-2} in 2004. During early growth periods, Q_N , Q_H , and Q_G were variable; the seasonal pattern was frequently disturbed by weather systems. Even as biomass steadily increased, Q_E showed irregular variations. Q_E increased from 30 to 80 Wm^{-2} in the early growth period of 2003 but was fairly stable at 20 Wm^{-2} in the early growth period of 2004. This result

can be explained by the relatively wet conditions in 2003 in contrast to the relatively dry conditions in 2004. During peak growth in the wetter year (July and August 2003), Q_N , Q_H , and Q_G ranged synchronously from 210–120, 140–65, and 16–3 Wm^{-2} , respectively. From early September to early October (the senescence period), Q_N , Q_H , and Q_G gradually decreased, reaching 47.0, 32.0, and 0 Wm^{-2} , respectively, in 2003. As biomass and LAI values decreased (Figure 5), Q_E decreased. This result differs from observations made in dense and tall grasslands (George and Shashi, 2001). The ratio of Q_E/Q_N and the Bowen ratio B_0 shows inter-annual change rather than seasonal variation. The former was stable around 0.4 during the main growth period of 2003, a moister summer, and dominantly fluctuated about 0.15 in the drier summer of 2004. These findings reveal the contribution of near-ground turbulence in the atmospheric layer to the energy partition produced by ground-surface conditions.

Because of distinct differences in ground surface conditions, we divided the year into a frozen-ground period (i.e. from when the ground surface became continuously frozen to when it thawed) and a non-frozen period. The latter period was further divided into three sub-periods according to the stage of grass growth: pre-growth, growth, and post-growth period. Heat budget components averaged over this periods are shown in Table II to quantify the seasonality of the heat budget and major biometeorological factors for each period.

Most energy flux parameters showed two extreme periods, one of which corresponded to the frozen-soil/snow-cover period. All the parameters in the growth period were different from those in other periods. Net radiation Q_N sharply increased after the pre-growth period and decreased as grass senescence began. The ground

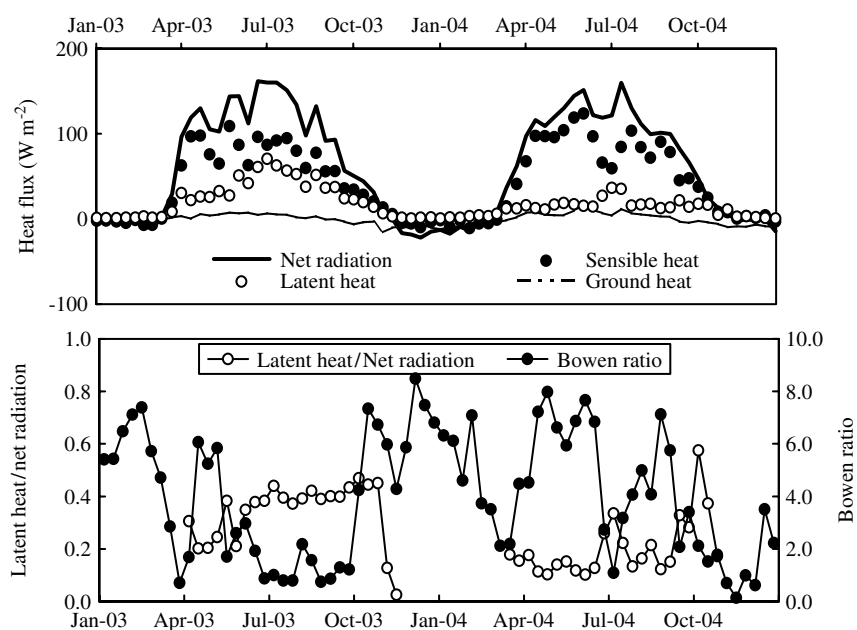
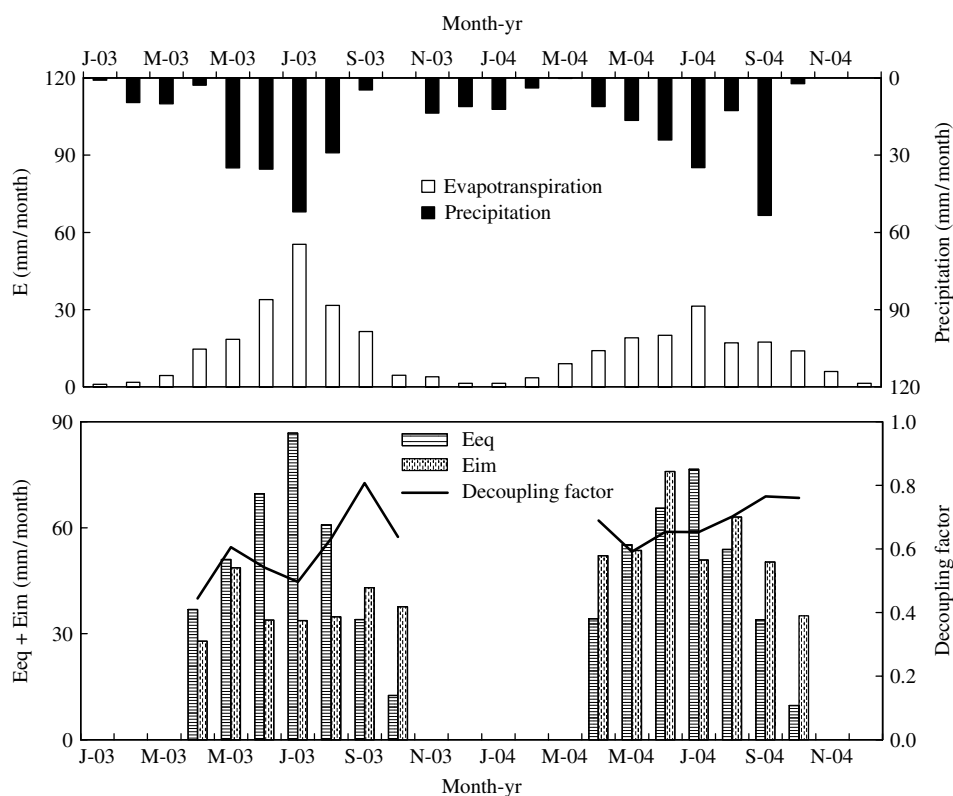


Figure 6. Seasonal variation of 10-day mean net radiation, sensible heat, latent heat, and ground heat flux at the study site during 2003 and 2004 (upper panel). Lower panel: 10-day mean values of partitioning of the latent heat flux to net radiation and the Bowen ratio for the 2003 and 2004 growth periods

Table II. Daily mean of solar radiation, energy budget components, and major bio-meteorological factors for each period

	Frozen-soil/snow-cover period	Non-frozen-soil/no snow-cover period		
		Pre-growth period	Growth period	Post-growth period
Global radiation (W/m^2)	116.6	233.4	234.8	158.7
Albedo	0.56	0.18	0.17	0.18
Q_N , (W/m^2)	4.9	114.0	117.0	48.6
Q_G/Q_N , (%)	-112	4.7	3.9	-5.8
Q_E/Q_N , (%)	108	17.7	27.5	37.0
Q_H/Q_N , (%)	104	77.6	68.6	68.9
Air temperature (at 2 m, $^{\circ}\text{C}$)	-17.8	3.1	12.3	0.9
Relative humidity (at 2 m, %)	67.1	50.4	57.5	58.5
Wind speed (at 2 m, m/s)	2.1	3.6	3.1	2.7
Vapour deficit (hPa)	0.8	4.8	8.2	4.1
Precipitation (total, mm)	64.0	14.1	297.8	1.2
E (total, mm)	49.3	26.6	265.9	12.1
LAI			0.67	
Decoupling factor	0.29	0.56	0.64	0.35

Figure 7. Seasonal variation of monthly evapotranspiration (E) and precipitation at the study site from 2003 to 2004 (upper panel, excluding snow sublimation). The lower panel shows monthly E_{eq} (equilibrium evaporation), E_{im} (imposed evaporation), and the decoupling factor

heat flux was positive (heat conductance to the deep soil) from the pre-growth period to the growth period; during other periods, the ground heat flux was negative. Q_H and Q_E showed fairly high values during the non-frozen period. In periods after the growth period (i.e. post-senescence and pre-growth), B_0 was lower in wetter years than in drier years. Q_E/Q_N and B_0 averaged 27.2% and 2.4, respectively, for the entire observation period. The frozen period was quite long in this fringe region of the cryosphere: 179 days in 2003 and 170 days

in 2004. This is an important period in the local water cycle and requires more detailed investigation than was done during the current study.

Seasonal variation of evapotranspiration coupled to precipitation

Evapotranspiration (E) was calculated using the aerodynamic method illustrated by Equations (3)–(8). Calculations were performed for snow-free periods in 2003 and 2004. The upper panel of Figure 7 shows the seasonal

variation of monthly E , precipitation at the study site from 2003 to 2004.

Clear seasonality became evident by comparing variations in precipitation and those of E . The E value was 170.0 mm for the snow-free period of 2003, coupling precipitation of 170.3 mm; in the corresponding snow-free period of 2004, E and precipitation was 128.6 and 142.8 mm respectively. Both E_{eq} and E_{im} showed similar seasonality to that of E (lower panel of Figure 7). The decoupling factor averaged 0.64 for the snow-free periods of the two years.

DISCUSSION

The sensitivity of evapotranspiration (E) to environmental factor can be summarized according to Jarvis and McNaughton (1986) by the following:

$$\frac{dE}{dgs} = (1 - \Omega) \frac{E}{gs} \quad (18)$$

where g_s is the bulk conductance of the ground surface (mm s^{-1}):

$$\frac{1}{g_s} = r_s = \frac{1}{g_a} + \frac{1}{g_c} \quad (19)$$

in which r_s is bulk surface resistance (mm s^{-1}). Ω is an index of the relative importance of the controlling factor (radiation, wind speed, vapour pressure deficit, or surface conductance) in the determination of E : the higher the Ω value, the lower indicates importance of the atmospheric and surface factors in the control of E , meaning that E is then mainly determined by net radiation. On the other hand, the lower the Ω values, indicates the greater the importance of atmospheric and surface factors in controlling E .

Evapotranspiration and radiation

Figure 8 presents the statistical results of Ω and corresponding mean evapotranspiration rate. It is clear that the frequency increase with increasing Ω , the occurrence of $\Omega > 0.8$ was 54.4%, implying the evapotranspiration process at the study site is coupled to the radiation forcing. A more comprehensive view of the effect of radiation can be

obtained by examining the distribution of the evapotranspiration rate in relation to Ω , which is shown in Figure 8. The higher evapotranspiration rate occurring with higher frequency of the larger Ω values reveals the importance of radiation forcing on evapotranspiration at the study site.

Atmospheric forcing

Ground surface conductance (g_s), which determined E directly, consisted of aero-conductance (g_a) and vegetation conductance (g_c), as given by formulas (18) and (19). The dependencies of g_a and g_c on environmental factors were in opposite directions (Figure 9); as Ω increases, evapotranspiration became more coupled with radiation forcing, and g_a increased while g_c decreased.

The magnitude of aero-conductance (g_a) depends on the aerodynamic properties of the surface and on wind speed; it is also a function of buoyancy (Monteith, 1995). In this study, g_a and g_c was calculated from Eddy covariance measurement using formulas (11) and (12). We parameterized g_a using wind stress (dU/dz) as shown in the left panel of Figure 10. An obvious relationship showed between g_a and dU/dz at the study plot:

$$g_a = 1.9748e^{1.412(\frac{dU}{dz})} \quad (20)$$

Both Kabat *et al.* (1997) and Hanan and Prince (1997) concluded that the vapour pressure deficit (d) was the

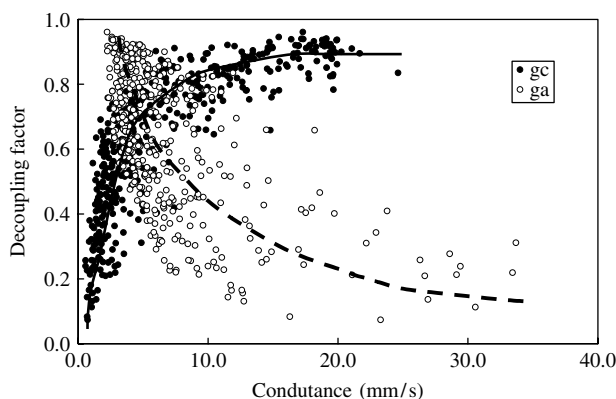


Figure 9. Variation of decoupling factor (Ω) versus aero-conductance (g_a) and vegetation conductance (g_c) at the study site in snow-free periods

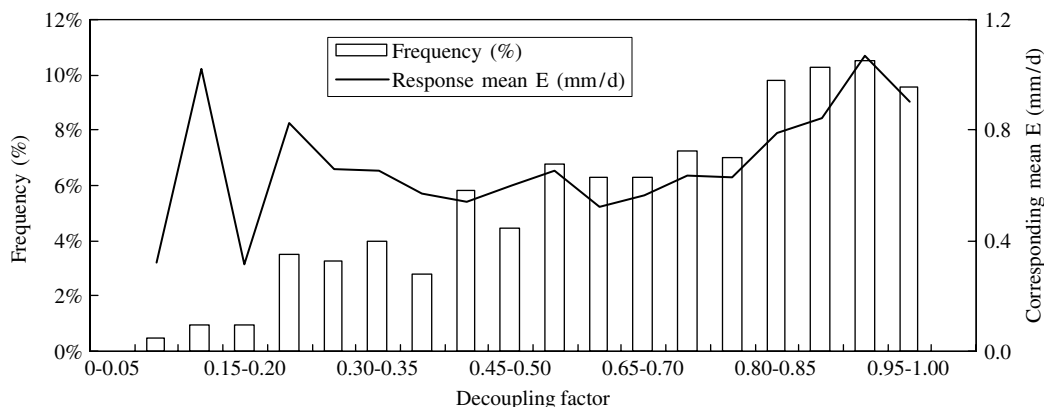


Figure 8. Frequency of the decoupling factor and corresponding mean evapotranspiration rate

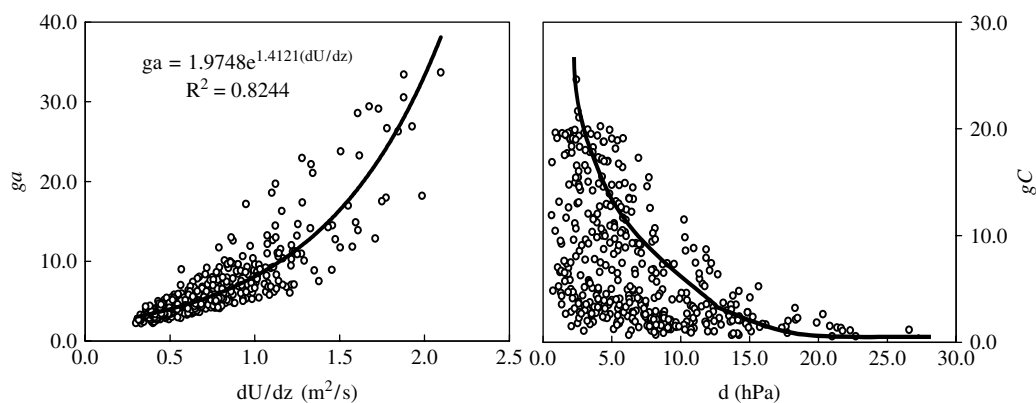


Figure 10. Variation of aero-conductance (g_a) versus wind stress (dU/dz), and vegetation conductance (g_C) versus vapour deficit (d) at the study site in snow-free periods

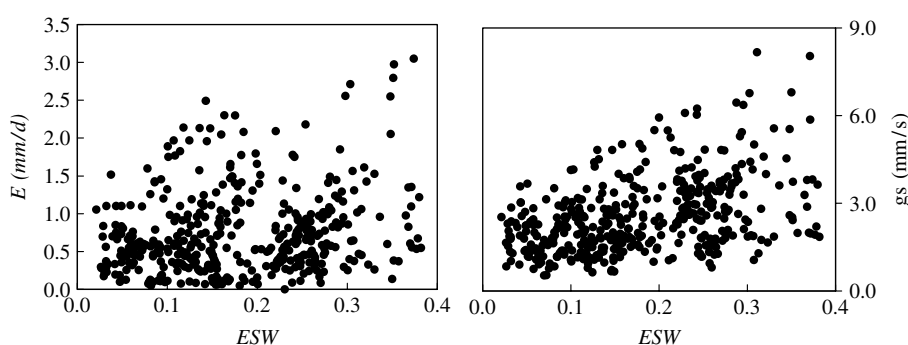


Figure 11. Variation of surface conductance (g_s , right panel) and evapotranspiration (E , left panel) versus ESW at the study site in snow-free periods

most significant environmental variable in explaining the variation in vegetation conductance (g_C) of the four most common species at the Hydrology-Atmosphere Pilot Experiment in the Sahel (HAPEX-Sahel) study area; this result was similar to that found for the present study site. We observed a strong trend of decreasing g_C with increasing d in snow-free periods (right panel of Figure 10). Similar conclusions may also be inferred from the results of Huntingford *et al.* (1995), who optimized a surface conductance model for fallow savannah. Further, g_C was also related to air temperature because of the obvious correlation between d and air temperature. However, d was the most important variable for the prediction of g_C at different time scales; d also explained 90% of the variance of g_C (Sommer *et al.*, 2002).

Surface-condition controls

Kurc and Small (2004) concluded that the correlation between E and soil moisture in the root zone was stronger than for an individual layer of semi-arid grassland. At our study site, a rough correlation of soil evaporation (E_{soil}) versus ESW can be seen in the right panel of Figure 11, despite soil moisture having been normalized to ESW . This finding points to a need for improved soil moisture observation techniques; our soil moisture values were deduced from TDR probe data.

Daly *et al.* (2004) simulated surface conductance (g_S) using Jarvis's formulation. They demonstrated that the simulated g_S compared well with measured values as

a function of ESW , and the general behaviour of g_S was also very well reproduced, with a plateau for well-watered conditions and a regular decay at lower soil water content. Our study site was locating dry region with ESW less than 0.4, the 'plateau' for well-watered conditions eventually missing (right panel of Figure 11). The 'regular decay' was found in our study site, showed only a tendency of g_S increasing with rising ESW .

Variation of the ratio of evapotranspiration to equilibrium evaporation (E/E_{eq}) versus LAI at the study site can be seen on left panel of Figure 12. Each point shows the 10-day mean value corresponding to the LAI data. For such sparse vegetation with a maximum LAI of 1.39, E/E_{eq} is not matched well to LAI, which varied generally versus LAI in wetter year of 2003 but irregularly in drier year of 2004 at the study site. E/E_{eq} can be expressed as a function of the surface soil moisture (Brutsaert, 1984), however, coefficient of the function must be different between wetter and drier year as shown in right panel of Figure 12. Saugier and Ader Katerji (1991) also concluded that in arid environments with low LAI the feedback between soil evaporation and transpiration becomes important and complex.

As a general conclusion, the bulk surface resistance ($r_S = 1/g_S$) to E depended mainly on the vapour pressure and was largely independent of wind stress. The close relationship between evapotranspiration and surface bulk resistance at the study site is shown in Figure 13, where the 10-day means of E versus bulk surface resistance

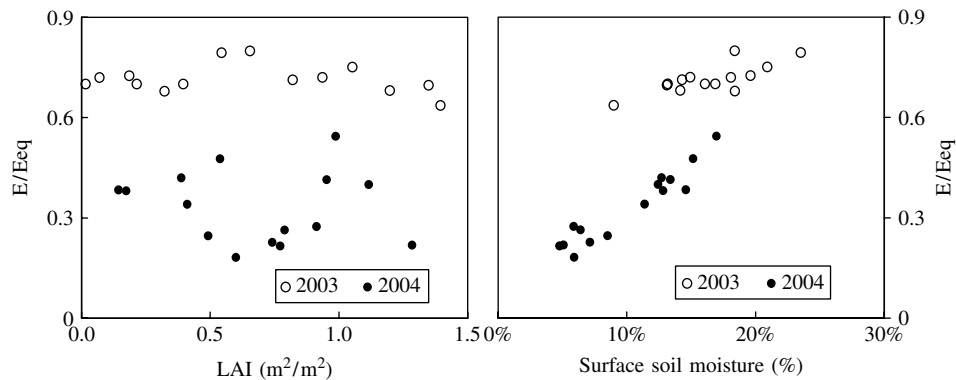


Figure 12. Variation of ratio of evapotranspiration to equilibrium evaporation (E/E_{eq}) versus the LAI (left panel) and versus surface soil moisture (right panel) at the study site in snow-free periods. Each point shows the 10-day mean

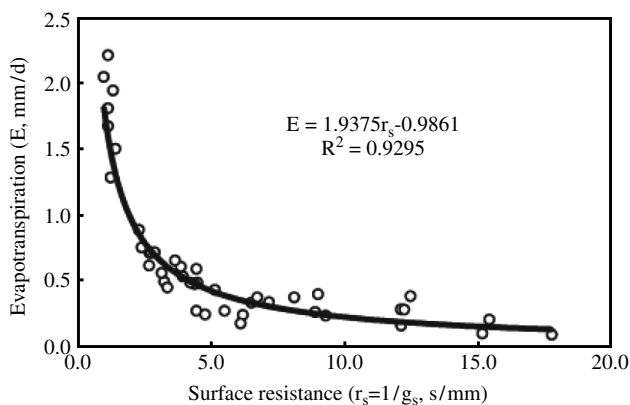


Figure 13. The dependence of the evapotranspiration (E) on the bulk surface resistance ($r_s = 1/g_s$)

described by Equations (19) and (20) have been plotted. The dependence can be fitted by the following function:

$$E = 1.9375(r_s)^{-0.9861}. \quad (21)$$

The form of Equation (21) is widely utilized in modelling the parameters of actual evapotranspiration (Wright *et al.*, 1995).

CONCLUDING REMARKS

The interaction processes between grassy land surfaces and the atmosphere can be summarized as follows: radiation absorption, evaporation from bare soil with water retained on the leaves, and transpiration and vertical diffusion of water through the soil. The partitioning of available land-surface energy into latent heat is a basic hydrological process connecting the vegetated land surface with the atmosphere. From the heat flux observations by both Eddy covariance and aerodynamic measurements taken during 2003 and 2004, the environmental controls on evapotranspiration were investigated for sparse grassland in Mongolia at a study site located on the southern periphery of the Eurasian cryosphere. The technique used to deduce aerodynamic parameters from Eddy covariance data produced satisfactory estimations of the evapotranspiration rate on a full seasonal scale, as verified by examination of the energy budget closure.

The study region is characterized by dry atmosphere, dry soil, and low grass production with a maximum LAI of 1.39. Evapotranspiration showed larger temporal variability coupling to precipitation.

The decoupling factor (Ω) was calculated to determine the relative importance of surface conductance and radiation in controlling evapotranspiration rates. Higher evapotranspiration rates were coupled to the higher frequencies of the larger Ω values, revealing the importance of radiation forcing on evapotranspiration at the study site. As Ω increased the aerodynamic conductance (g_a) increased correspondingly but the vegetation conductance (g_c) decreased. The aero-conductance (g_a) was well matched to the wind stress (dU/dz) through an exponential function. The value of g_c decreased very clearly as the vapour pressure deficit increased; g_c was also related to air temperature because of the obvious correlation between d and air temperature. Although grass cover was sparse at the study site, the effect of soil moisture on E and g_s could not be deduced beyond the observation of a vague tendency towards a relationship, perhaps caused by errors in soil moisture observations or soil moisture being too low for accurate measurement.

On the 10-day-interval time scale, the effect of vegetation cover on evapotranspiration was insignificant comparing to that of surface soil moisture. However, more intensive observation (e.g. detecting diurnal trends in the LAI) should clarify surface controls on evapotranspiration for sparse grassland such as that at the study site. Changes in soil evaporation, related to precipitation, mainly caused the very large inter-annual differences in E/E_{eq} .

ACKNOWLEDGEMENTS

Grateful thanks are extended to Drs D. Azzaya, G. Davaa, and Mr Ts. Ganbold for their help and cooperation with our field work in Mongolia.

REFERENCES

- Alves I, Pereira LS. 2000. Modeling surface resistance from climatic variables? *Agricultural Water Management* **42**: 371–385.

- Berevena IA. 1992. Peculiarities of studies and methods of assessment of climatic resources of complex ecosystems of Mongolia. In *Ecology and Nature Management in Mongolia*, Dorofeyuk NI (ed). GUGK MPR: Ulaanbaatar (In Russian); 25–32.
- Brutsaert W. 1984. *Evaporation into the Atmosphere*. Kluwer Academic: Reidel, Boston, MA; 216.
- Calvet JC. 2000. Investigating soil and atmospheric plant water stress using physiological and micrometeorological data. *Agricultural and Forest Meteorology* **103**: 229–247.
- Daly E, Porporato A, Rodriguez-Iturbe I. 2004. Coupled dynamics of photosynthesis, transpiration, and soil water balance. Part I: upscaling from hourly to daily level. *Journal of Hydrometeorology* **5**: 546–558.
- Desborough C, Pitman A, Irannejad P. 1996. Analysis of the relationship between bare soil evaporation and soil moisture simulated by 13 land surface schemes for a simple non-vegetated site. *Global and Planetary Change* **13**: 47–56.
- Dirmeyer PA. 1994. Vegetation as a feedback mechanism in midlatitude drought. *Journal of Climate* **7**: 1463–1483.
- Flanagan LB, Wever LA, Carlson PJ. 2002. Seasonal and interannual variation in carbon dioxide exchange and carbon balance in a northern temperate grassland. *Global Change Biology* **8**: 599–615.
- George GB, Shashi BV. 2001. Prairie growth, PAR albedo and seasonal distribution of energy fluxes. *Agricultural and Forest Meteorology* **107**: 227–240. 25.
- Grelle A, Lindroth A, Molder M. 1999. Seasonal variation of boreal forest surface conductance and evaporation. *Agricultural and Forest Meteorology* **98–99**: 563–578.
- Hanan NP, Prince SD. 1997. Stomatal conductance of west central supersite vegetation in Hapex-Sahel: measurements and empirical models. *Journal of Hydrology* **188–189**: 536–562.
- Huntingford C, Allen SJ, Harding RJ. 1995. An intercomparison of single and dual-source vegetation—atmosphere transfer models applied to transpiration from Sahelian savannah. *Boundary-Layer Meteorology* **74**: 397–418.
- Ishikawa M, Sharkhuu N, Zhang Y, Kadota T, Ohata T. 2005a. Ground thermal and moisture conditions at the southern boundary of discontinuous permafrost, Mongolia. *Permafrost and Periglacial Processes* **16**: 209–216.
- Ishikawa M, Zhang Y, Kadota T, Tetsuo Ohata T. 2006. Hydrothermal regimes of dry active layer. *Water resources Research* **42**. DOI: 10.1029/2005WR004200.
- Jarvis PG, McNaughton KG. 1986. Stomatal control of transpiration. *Advances in Ecological Research* **15**: 1–49.
- Jones HG. 1992. *Plants and Microclimate*, 2nd edn. Cambridge University Press; 156–157.
- Kabat P, Dohnan AJ, Elbers JA. 1997. Evaporation, sensible heat and canopy conductance of fallow savannah and patterned woodland in the Sahel. *Journal of Hydrology* **188–189**: 494–515.
- Knapp AK, Smith MD. 2001. Variation among biomes in temporal dynamics of aboveground primary production. *Science* **291**: 481–484.
- Kurc SA, Small EE. 2004. Dynamics of evapotranspiration in semiarid grassland and shrubland ecosystems during the summer monsoon season, central New Mexico. *Water Resources Research* **40**: W09305, doi:10.1029/2004WR003068.
- Ma X, Yasunari T, Ohata T, Natsagdorj L, Davaa G, Oyunbaatar D. 2003. Hydrological regime analysis of the Selenge River Basin, Mongolia. *Hydrological Processes* **17**: 2929–2945.
- Mahfouf J, Cîret C, Ducharne A, Irannejad P, Noilhan J, Shao Y, Thornton P, Xue Y, Yang Z. 1996. Analysis of transpiration results from the RICE and PILPS workshop. *Global and Planetary Change* **13**: 73–88.
- Mo X, Liu S. 2001. Simulating evapotranspiration and photosynthesis of winter wheat over the growing season. *Agricultural and Forest Meteorology* **109**: 203–222.
- Monteith JL. 1995. Accommodation between transpiring vegetation and the convective boundary layer. *Journal of Hydrology* **166**: 251–263.
- Monteith JL, Unsworth MH. 1990. *Principles of Environmental Physics*, 2nd edn. Edward Arnold: London, 291.
- Noilhan J, Planton S. 1989. A simple parameterization of land surface processes for meteorological models. *Monthly Weather Review* **117**: 536–549.
- Noy-Meir I. 1973. Desert ecosystems: Environment and producers. *Annual Review of Ecology and Systematics* **4**: 25–51.
- Pielke RS, Avissar R, Raupach M, Dolman AJ, Zeng X, Denning AS Sr. 1998. Interactions between the atmosphere and terrestrial ecosystems: influence on weather and climate. *Global Change Biology* **4**: 461–475.
- Rodriguez-Iturbe I. 2000. Ecohydrology: a hydrological perspective of climate—soil—vegetation dynamics. *Water Resources Research* **36**(1): 3–9.
- Saugier B, Ader Katerji N. 1991. Some plant factors controlling evapotranspiration. *Agricultural and Forest Meteorology* **54**: 263–277.
- Schulze ED, Kelliher FM, Körner C, Lloyd J, Leuning R. 1994. Relationships among maximum stomatal conductance, ecosystem surface conductance, carbon assimilation rate, and plant nitrogen nutrition: a global ecology scaling exercise. *Annual Review of Ecology and Systematics* **25**: 629–660.
- Sellers PJ, Bounoua GJ, Collatz DA, Randall DA, Dazlich SO, Los JA, Berry I, Fung CJ, Tucker CB, Jensen TG. 1996. Comparison of radiative and physiological effects of doubled atmospheric CO₂ on climate. *Science* **271**: 1402–1406.
- Sharkhuu N. 2001. Dynamics of permafrost in Mongolia. *Tohoku Geophysical Journal* **36**(2): 91–99.
- Shirley AK, Eric ES. 2004. Dynamics of evapotranspiration in semiarid grassland and shrubland ecosystems during the summer monsoon season, central New Mexico. *Water Resources Research* **40**: W09305, doi:10.1029/2004WR003068.
- Shuttleworth WJ, Wallace JS. 1985. Evaporation from sparse crops—an energy combination theory. *Quarterly Journal of the Royal Meteorological Society* **111**: 839–855.
- Sommer R, Tatiana D, de Abreu Sa, Vielhauer K, Carioca A, Fölster H, Vlek PLG. 2002. Transpiration and canopy conductance of secondary vegetation in the eastern Amazon. *Agricultural and Forest Meteorology* **112**: 103–121.
- Steduto P, Hsiao TC. 1998. Maize canopies under two soil water regimes: I. Diurnal patterns of energy balance, carbon dioxide flux, and canopy conductance. *Agricultural and Forest Meteorology* **89**: 169–184.
- Villalobos FJ, Orgaz F, Testi L, Fereres E. 2000. Measurement and modeling of evapotranspiration of olive (*Olea europaea* L.) orchards. *European Journal of Agronomy* **13**: 155–163.
- Viterbo P, Beljaars ACM. 1995. An improved land parameterization scheme in the ECMWF model and its validation. *Journal of Climate* **8**: 2716–2748.
- Wilson KB, Baldocchi DD. 2000. Factors controlling evaporation and energy partitioning beneath a deciduous forest over an annual cycle. *Agricultural and Forest Meteorology* **102**: 83–103.
- Woodward FI, Smith TM. 1994. Global photosynthesis and stomatal conductance: modeling the controls by soil and climate. *Botanical Resources* **20**: 1–41.
- Wright IR, Manzi AO, da Rocha HR. 1995. Surface conductance of amazonian pasture: model application and calibration for canopy climate. *Agricultural and Forest Meteorology* **75**: 51–70.
- Yokoyama K, Ohno H, Kominami Y, Inoue S, Kawakata T. 2003. Performance of Japanese precipitation gauges in winter. *Seppyo* **65**: 303–316.
- Zhang Y, Ohata T, Yang D, Davaa G. 2004. Bias correction of daily precipitation measurements for Mongolia. *Hydrological Processes* **18**: 2991–3005.